Technium Vol. 4, No. 7 pp.22-39 (2022)
ISSN: 2668-778X
www.techniumscience.com

Analytical Study of Dynamic and Vibrational of Composite Shell with Piezoelectric Layer using GDQM Method

Amin Moslemi Petrudi [1*] , Masoud Rahmani [1] , Ionut Cristian Scurtu [2]

[1] Department of Mechanical Engineering, Imam Hussein University, Tehran, Iran
[2] Naval Academy Mircea cel Batran Constanta

Abstract

Piezoelectric materials, due to their electromechanical coupling properties, are widely used as actuators and sensors in intelligent structures to control vibrations and bends of multilayer sheets with piezoelectric layers. In this paper, the response of free vibrations of a multilayer composite shell with the new Generalized Differential Quadrature Method (GDQM) for different boundary conditions is investigated. The governing equations are obtained by assuming first-order shear theory and using Hamilton's principle. The generalized quadrature differential method is used to solve the obtained equations. To use this method, coding has been done in MATLAB software. Due to the same thickness of the layers, as the number of composite layers increases and the total thickness is constant, the thickness of each layer decreases, and consequently the thickness of the piezoelectric layer decreases. Comparing the results of this method with the work of other researchers shows that this method has good accuracy.

Keywords: Composite shell, Piezoelectric, material, Hamilton's principle, GDQM Method.

1 Introduction

Combining composite materials with piezoelectric materials can provide very good properties for use in various electromechanical systems as sensors and operators. Piezoelectric properties were scientifically expressed by Pierre and Jacques Corey in 1880. They described the direct and reverse effect as the basis of piezoelectricity. If the operating frequency of the system reaches the value of the natural frequency of the system, the deformations will be very large and the structure will be destroyed. In this study, the effect of mechanical and geometric parameters of vibrational behavior of a three-layer electric scaling sheet is investigated. Research on past references can further demonstrate the need for this research. Jay-Hong Han et al. [1] analyzed a composite sheet with a piezoelectric layer of sensor and operator to control vibrations using layered theory. Plate theory, it is concluded that the developed model can describe more realistic smart composite plates with distributed piezoelectric actuators. Narayanan et al. [2] performed a finite element method for modeling intelligent structures with a piezoelectric layer for active control with operator and sensor layers. Heidary et al. [3] performed the forced vibration control of a thermoplastic composite sheet with piezoelectric. Based on the classical theory of sheets, they derived the equations of motion of the sheet around the joint using Hamilton's principle. Zhang et al. [5] investigated optimal shape control of CNT reinforced functionally graded composite plates using piezoelectric patches. Sharma et al. [6] using piezoelectric layers as sensors and the operator investigated the vibration control of carbon nanotube-reinforced composite sheets.

[*] Corresponding author. Tel.: 01142565736
E-mail address: msrahmani@ihu.ac.ir

Ansari et al. [7] used the Reissner-Mindlin strain gradient theory for Nanoshells of functional materials. length scale parameters, material properties, temperature difference, and compressive axial loads on the natural frequencies, critical flow velocities, and instability of the system. Farzam-Rad et al. [8] used this method and theory of quasi-three-dimensional shear deformation for sheets of functional materials. Chen et al. [9] proposed a model for the piezoelectric thermomechanical coupling, which also used the Hamilton method and the Rayleigh method to obtain the governing nonlinear equations. And they solved the equations by the harmonic balance method and compared the results with the Runge–Kutta numerical method. They found that the frequency increases with increasing temperature while the resonance amplitude decreases. In this research, to evaluate the efficiency and accuracy of the analysis method from the solution of piezoelectric composite multilayer sheets is investigated. The generalized differential squares method is used to discretize the governing equations and boundary conditions, to improve the differential squares method, and also to calculate the weight coefficients. In recent years, this method has been considered by researchers in various branches of science due to its high accuracy and convergence rate. The nature of the method of differential squares is a partial derivative of a uniform function concerning a variable that is approximated by the weighted sum of the values of the function at all discrete points in that direction. The weight coefficients associated with it are not problem-specific and depend only on the network points and the derivative order. In this method, network points are selected optionally and without any limitation. The three-layer sheet under study consists of a composite layer and two connected layers at the top and bottom made of piezoelectric calibrated materials. Changes in mechanical and electrical properties in the core and equipped layers are considered in general and differently. Vibrating characteristics and flexural behavior of the structure can be controlled by using piezoelectric calibrated materials. Safarpour et al. [10] The validity of the current approach is assessed by comparing its numerical results with those available in the literature. Especial attention is drawn to the role of GPLs weight fraction, patterns of GPLs distribution through the thickness direction, geometrical parameters such as semi-vertex angle, length to the mid-radius ratio on natural frequencies, and bending characteristics. Habibi et al. [11] investigated vibration analysis of a high-speed rotating GPLRC nanostructure coupled with a piezoelectric actuator. The results of the current study are useful for the design of materials science, micro-electro-mechanical systems, and nanoelectromechanical systems such as nano actuators and nanosensors. Ebrahimi et al. [12] investigated frequency characteristics of a GPL-reinforced composite microdisk coupled with a piezoelectric layer. Ramegowda et al. [13] investigated finite element analysis of a thin piezoelectric .Numerical results are given for various electrical configurations of actuators and sensors to validate the present method. Comparison with an exact solution illustrates the accuracy, efficiency, and capability of the developed solid direct and shell inverse-piezoelectric analysis coupled with a pseudo-direct-piezoelectric evaluation method to capture the sensor and actuator response of a thin piezoelectric bimorph with a metal shim.

2 Problem statement and Governing Equations

According to the first-order shear theory for plates, as Figure 1 shows, the transverse normality does not remain perpendicular to the center plate after the plate deforms. The reason for this is to consider the effects of shear stresses on deformation. In thick sheets and plates, shear stresses will increase significantly, and therefore in the analysis of thick plates, a theory capable of considering the effects of these stresses should be used. For this purpose, will use the first-order shear theory [1]. Figure 1 shows the sheet under consideration in the problem.

Technium Vol. 4, No. 7 pp.22-39 (2022)
ISSN: 2668-778X
www.techniumscience.com

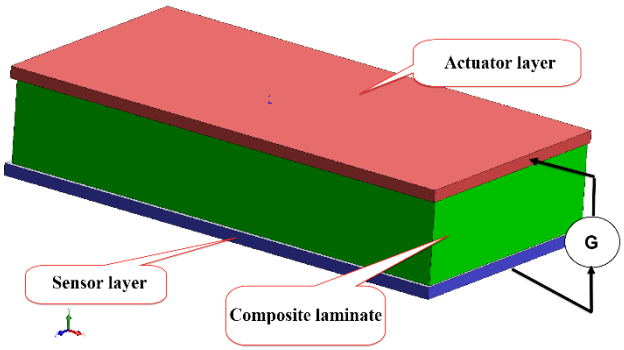

a) Schematic of a composite sandwich sheet with piezoelectric layers.

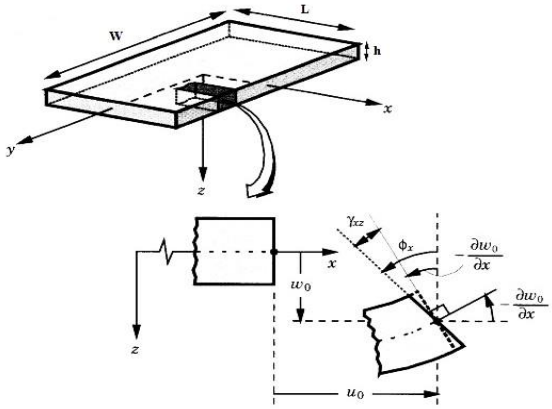

b) Deformation of a plate considering the shear strain energy [1].

Figure 1.The sheet under consideration in the problem.

According to Figure 1, the displacement field will be as follows:

$$\begin{aligned} u(x,y,z,t) &= u_0(x,y,t) + z\psi_x(x,y,t) \\ v(x,y,z,t) &= v_0(x,y,t) + z\psi_y(x,y,t) \\ w(x,y,z,t) &= w_0(x,y,t) \end{aligned} \tag{1}$$

That, u , v , w In order of the components of the displacement at any point in the desired direction x , z , y . u_0 , v_0 , w_0 also to the components of displacement on-page $Z=0$. ψ_x and ψ_y respectively, they indicate a transverse vertical rotation around the y and x axis and will be equal to:

$$\psi_x = \frac{\partial u}{\partial z} \tag{2}$$

$$\psi_y = \frac{\partial v}{\partial z} \tag{3}$$

If the beam or plate is thin and as a result, the transverse shear strains are small, which will lead to the perpendicular cross-section of the beam or plate to the neutral plate, we will have:

$$\psi_x = -\frac{\partial w}{\partial x} \tag{4}$$

$$\psi_y = -\frac{\partial w}{\partial y} \tag{5}$$

In this study, all values of u_0, v_0, w_0, ψ_x, ψ_y the unknown will be considered a problem. The strain-displacement relations will be as follows:

$$\begin{aligned}
\varepsilon_x &= \frac{\partial u}{\partial x} = \varepsilon_x^0 + z\kappa_x \\
\varepsilon_y &= \frac{\partial v}{\partial y} = \varepsilon_y^0 + z\kappa_y \\
\varepsilon_z &= \frac{\partial w}{\partial z} = 0 \\
\gamma_{xy} &= \frac{\partial u}{\partial y} + \frac{\partial v}{\partial x} = \gamma_{xy}^0 + z\kappa_{xy} \\
\gamma_{yz} &= \gamma_{yz}^0 \\
\gamma_{xz} &= \gamma_{xz}^0
\end{aligned} \tag{6}$$

That:

$$\begin{aligned}
\varepsilon_x^0 &= \frac{\partial u_0}{\partial x} & \kappa_x &= \frac{\partial \psi_x}{\partial x} \\
\varepsilon_y^0 &= \frac{\partial v_0}{\partial y} & \kappa_y &= \frac{\partial \psi_y}{\partial y} \\
\gamma_{xy}^0 &= \frac{\partial u_0}{\partial y} + \frac{\partial v_0}{\partial x} & \kappa_{xy} &= \frac{\partial \psi_x}{\partial y} + \frac{\partial \psi_y}{\partial x} \\
\gamma_{yz}^0 &= \frac{\partial w_0}{\partial y} + \psi_y \\
\gamma_{xz}^0 &= \frac{\partial w_0}{\partial x} + \psi_x
\end{aligned} \tag{7}$$

Tension-strain relations for layer k they will be as follows:

$$\begin{Bmatrix} \sigma_x \\ \sigma_y \\ \sigma_{xy} \end{Bmatrix}^{(k)} = \begin{bmatrix} \bar{Q}_{11} & \bar{Q}_{12} & \bar{Q}_{16} \\ \bar{Q}_{12} & \bar{Q}_{22} & \bar{Q}_{26} \\ \bar{Q}_{16} & \bar{Q}_{26} & \bar{Q}_{66} \end{bmatrix}^{(k)} \left(\begin{Bmatrix} \varepsilon_x^0 \\ \varepsilon_y^0 \\ \gamma_{xy}^0 \end{Bmatrix} + z \begin{Bmatrix} \kappa_x \\ \kappa_y \\ \kappa_{xy} \end{Bmatrix} \right) \tag{8-a}$$

$$\begin{Bmatrix} \sigma_{yz} \\ \sigma_{xz} \end{Bmatrix}^{(k)} = \begin{bmatrix} \bar{Q}_{44} & \bar{Q}_{45} \\ \bar{Q}_{45} & \bar{Q}_{55} \end{bmatrix}^{(k)} \begin{Bmatrix} \gamma_{yz}^0 \\ \gamma_{xz}^0 \end{Bmatrix} \tag{8-b}$$

That $\bar{Q}_{ij}^{(k)}$ decreased stiffness of k the layer [1]. We will have motion equations for pages according to Hamilton's principle:

Technium Vol. 4, No. 7 pp.22-39 (2022)
ISSN: 2668-778X
www.techniumscience.com

$$\int_0^T \left(\delta U + \delta V - \delta K\right) dt = 0 \tag{9}$$

That:
Strain energy changes, δU , Potential energy changes, δV and Kinetic energy changes, δK . These changes will be equal to:

$$\delta U = \int_0^W \int_0^L \int_{-h/2}^{h/2} \Big[\sigma_x \left(\delta\varepsilon_x^0 + z\delta\kappa_x\right) + \sigma_y \left(\delta\varepsilon_y^0 + z\delta\kappa_y\right) + \sigma_{xy}\left(\delta\gamma_{xy}^0 + z\delta\kappa_{xy}\right) + \sigma_{yz}\delta\gamma_{yz}^0 + \sigma_{xz}\delta\gamma_{xz}^0\Big] dzdxdy \tag{10}$$

$$\delta V = \int_0^W \int_0^L \int_{-h/2}^{h/2} q(x,y,t)\ dzdxdy \tag{11}$$

$$\delta K = \int_0^W \int_0^L \int_{-h/2}^{h/2} \rho\Big[\left(\dot{u}_0 + z\dot{\psi}_x\right)\left(\delta\dot{u}_0 + z\delta\dot{\psi}_x\right) + \left(\dot{v}_0 + z\dot{\psi}_y\right)\left(\delta\dot{v}_0 + z\delta\dot{\psi}_y\right) + \dot{w}_0\delta\dot{w}_0\Big] dzdxdy \tag{12}$$

According to Figure 1, L, W ,h the length, width, and thickness of the page, respectively, and ρ, the density is related to the layer from which the integral is taken in terms of thickness. $q(x,y,t)$ the extensive external load applied to the system. The following are the definitions of force and moment, and Figure 2 shows these results for a rectangular plate.

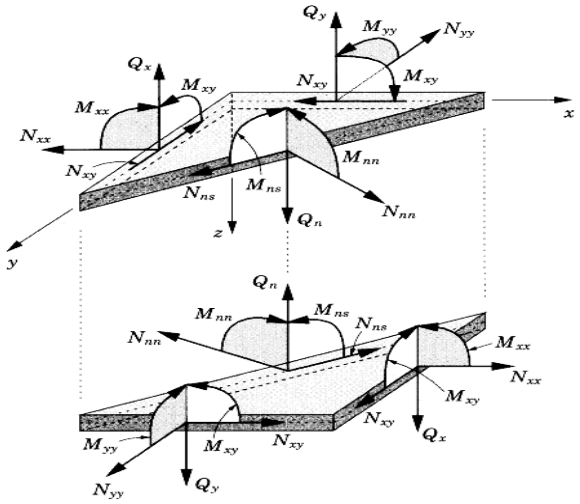

Figure 2. Force and moment result in planes parallel to the coordinate axes [1].

These results will be equal to:

$$\begin{Bmatrix} N_x \\ N_y \\ N_{xy} \end{Bmatrix} = \sum_{k=1}^{3} \int_{z_k}^{z_{k+1}} \begin{Bmatrix} \sigma_x \\ \sigma_y \\ \sigma_{xy} \end{Bmatrix}^{(k)} dz \tag{13-a}$$

$$\begin{Bmatrix} M_x \\ M_y \\ M_{xy} \end{Bmatrix} = \sum_{k=1}^{3} \int_{z_k}^{z_{k+1}} \begin{Bmatrix} \sigma_x \\ \sigma_y \\ \sigma_{xy} \end{Bmatrix}^{(k)} zdz \tag{13-b}$$

$$\begin{Bmatrix} Q_x \\ Q_y \end{Bmatrix} = K_s \sum_{k=1}^{3} \int_{z_k}^{z_{k+1}} \begin{Bmatrix} \sigma_{xz} \\ \sigma_{yz} \end{Bmatrix}^{(k)} dz \tag{13-c}$$

Technium Vol. 4, No. 7 pp.22-39 (2022)
ISSN: 2668-778X
www.techniumscience.com

In Equations (6) and (7), the cross-sectional strains of the whole plate are in the direction of constant thickness, which according to relation (8) the cross-sectional stresses will also be obtained in the direction of constant thickness. According to the introductory theory for homogeneous beams, the changes in cross-sectional stresses in the direction of thickness are parabolic. In beams, plates, and composite shells, the changes in cross-sectional stresses along the thickness will be at minimum second degrees. The difference between the actual stresses and the stresses obtained from the first-order theory is corrected by multiplying the shear force results by a constant number K_s. Various values have been reported for this coefficient, in which the value $5/6$ for Ks will be obtained [1].
By placing relations (8) in relations (13):

$$\begin{Bmatrix} N_x \\ N_y \\ N_{xy} \end{Bmatrix} = \begin{bmatrix} A_{11} & A_{12} & A_{16} \\ A_{21} & A_{22} & A_{26} \\ A_{61} & A_{62} & A_{66} \end{bmatrix} \begin{Bmatrix} \varepsilon_x^0 \\ \varepsilon_y^0 \\ \gamma_{xy}^0 \end{Bmatrix} + \begin{bmatrix} B_{11} & B_{12} & B_{16} \\ B_{21} & B_{22} & B_{26} \\ B_{61} & B_{62} & B_{66} \end{bmatrix} \begin{Bmatrix} \kappa_x \\ \kappa_y \\ \kappa_{xy} \end{Bmatrix} \tag{14-a}$$

$$\begin{Bmatrix} M_x \\ M_y \\ M_{xy} \end{Bmatrix} = \begin{bmatrix} B_{11} & B_{12} & B_{16} \\ B_{21} & B_{22} & B_{26} \\ B_{61} & B_{62} & B_{66} \end{bmatrix} \begin{Bmatrix} \varepsilon_x^0 \\ \varepsilon_y^0 \\ \gamma_{xy}^0 \end{Bmatrix} + \begin{bmatrix} D_{11} & D_{12} & D_{16} \\ D_{21} & D_{22} & D_{26} \\ D_{61} & D_{62} & D_{66} \end{bmatrix} \begin{Bmatrix} \kappa_x \\ \kappa_y \\ \kappa_{xy} \end{Bmatrix} \tag{14-b}$$

$$\begin{Bmatrix} Q_x \\ Q_y \end{Bmatrix} = K_s \begin{bmatrix} A_{55} & A_{54} \\ A_{45} & A_{44} \end{bmatrix} \begin{Bmatrix} \gamma_{xz}^0 \\ \gamma_{yz}^0 \end{Bmatrix} \tag{14-c}$$

That:

$$(A_{ij}, B_{ij}, D_{ij}) = \int_{-h/2}^{h/2} \bar{Q}_{ij}(1, z, z^2) dz,\ i, j = 1, 2, 6 \tag{15}$$

By placing relations (6) and (7) in relations (14), the results will be obtained according to the components of displacement. By substituting relations (14) in relations (10) to (12) and substituting the answer obtained in relation (9):

$$\begin{aligned} &\int_0^T \int_0^W \int_0^L \Big[N_x \delta\varepsilon_x^0 + M_x \delta\kappa_x + N_y \delta\varepsilon_y^0 + M_y \delta\kappa_y \\ &+ N_{xy} \delta\gamma_{xy}^0 + M_{xy} \delta\kappa_{xy} + Q_x \delta\gamma_{xz}^0 + Q_y \delta\gamma_{yz}^0 + q\delta w_0 \\ &- I_0 \left(\dot{u}_0 \delta\dot{u}_0 + \dot{v}_0 \delta\dot{v}_0 + \dot{w}_0 \delta\dot{w}_0 \right) \\ &- I_1 \left(\dot{\psi}_x \delta\dot{u}_0 + \dot{\psi}_y \delta\dot{v}_0 + \dot{u}_0 \delta\dot{\psi}_x + \dot{v}_0 \delta\dot{\psi}_y \right) \\ &- I_2 \left(\dot{\psi}_x \delta\dot{\psi}_x + \dot{\psi}_y \delta\dot{\psi}_y \right) \Big] \, dxdydt = 0 \end{aligned} \tag{16}$$

That:

$$I_i = \int_{-h/2}^{h/2} \rho z^i dz = \sum_{k=1}^{3} \int_{z_k}^{z_{k+1}} \rho^{(k)} z^i dz,\ i = 0, 1, 2 \tag{17}$$

By substituting relations (7) for relations (16) and (17), will have an integral part:

$$\int_0^T\int_0^W\int_0^L\Bigg\{-\left(\frac{\partial N_x}{\partial x}+\frac{\partial N_{xy}}{\partial y}-I_0\frac{\partial^2 u_0}{\partial t^2}-I_1\frac{\partial^2\psi_x}{\partial t^2}\right)\delta u_0$$
$$-\left(\frac{\partial N_{xy}}{\partial x}+\frac{\partial N_y}{\partial y}-I_0\frac{\partial^2 v_0}{\partial t^2}-I_1\frac{\partial^2\psi_y}{\partial t^2}\right)\delta v_0$$
$$-\left(\frac{\partial M_x}{\partial x}+\frac{\partial M_{xy}}{\partial y}-Q_x-I_1\frac{\partial^2 u_0}{\partial t^2}-I_2\frac{\partial^2\psi_x}{\partial t^2}\right)\delta\psi_x$$
$$-\left(\frac{\partial M_{xy}}{\partial x}+\frac{\partial M_y}{\partial y}-Q_y-I_1\frac{\partial^2 v_0}{\partial t^2}-I_2\frac{\partial^2\psi_y}{\partial t^2}\right)\delta\psi_y \qquad (18)$$
$$-\left[\frac{\partial Q_x}{\partial x}+\frac{\partial Q_y}{\partial y}+q(x,y,t)-I_0\frac{\partial^2 w_0}{\partial t^2}\right]\delta w_0\Bigg\}\,dxdydt$$
$$+\int_0^T\int_0^W\left[N_x\delta u_0+M_x\delta\psi_x+N_{xy}\delta v_0+M_{xy}\delta\psi_y+Q_x\delta w_0\right]_{x=0}^{x=L}dydt$$
$$+\int_0^T\int_0^L\left[N_{xy}\delta u_0+M_{xy}\delta\psi_x+N_y\delta v_0+M_y\delta\psi_y+Q_y\delta w_0\right]_{y=0}^{y=W}dxdt=0$$

Using the Fundamental lemma of the calculus of variation, the equations of motion will be obtained as follows:

$$\frac{\partial N_x}{\partial x}+\frac{\partial N_{xy}}{\partial y}=I_0\frac{\partial^2 u_0}{\partial t^2}+I_1\frac{\partial^2\psi_x}{\partial t^2}$$
$$\frac{\partial N_{xy}}{\partial x}+\frac{\partial N_y}{\partial y}=I_0\frac{\partial^2 v_0}{\partial t^2}+I_1\frac{\partial^2\psi_y}{\partial t^2}$$
$$\frac{\partial Q_x}{\partial x}+\frac{\partial Q_y}{\partial y}+q(x,y,t)=I_0\frac{\partial^2 w_0}{\partial t^2} \qquad (19)$$
$$\frac{\partial M_x}{\partial x}+\frac{\partial M_{xy}}{\partial y}-Q_x=I_1\frac{\partial^2 u_0}{\partial t^2}+I_2\frac{\partial^2\psi_x}{\partial t^2}$$
$$\frac{\partial M_{xy}}{\partial x}+\frac{\partial M_y}{\partial y}-Q_y=I_1\frac{\partial^2 v_0}{\partial t^2}+I_2\frac{\partial^2\psi_y}{\partial t^2}$$

The piezoelectric relations are given in the following index [14]:

$$\sigma_{ij}=c_{ijkl}\,\varepsilon_{kl}-e_{kij}\,E_k$$
$$D_i=e_{ikl}\,\varepsilon_{kl}+\epsilon_{ik}\,E_k \qquad (20)$$

Due to the thinness of the piezo layer, will neglect the shear term in this layer and as a result, in relations (12), we will have for the piezoelectric layer:

$$\sigma_{xx}=c_{11}\varepsilon_{xx}-e_{31}\,E_z$$
$$\begin{Bmatrix}D_x\\D_z\end{Bmatrix}=\begin{pmatrix}\epsilon_{11}&0\\0&\epsilon_{33}\end{pmatrix}\begin{Bmatrix}E_x\\E_z\end{Bmatrix} \qquad (21)$$
$$+\begin{pmatrix}0&e_{15}\\e_{31}&0\end{pmatrix}\begin{Bmatrix}\varepsilon_{xx}\\\varepsilon_{xz}\end{Bmatrix}$$

Due to the thinness of the piezoelectric layer, electrical displacement in the other two directions of the piezoelectric layer can be neglected. Eventually, the piezoelectric relationships of the layers will be reduced as follows:

$$\sigma_{xx}=c_{11}\varepsilon_{xx}-e_{31}\,E_z$$
$$D_z=e_{31}\,\varepsilon_{xx}+\epsilon_{33}\,E_z \qquad (22)$$

Since there is no external electrical charge in the sensor, the electrical displacement of this layer will be zero in line with the thickness; so:

$$D_z = e_{31}\left(\frac{\partial u_0}{\partial_x} + z\,\frac{\partial_{\psi(x)}}{\partial_x}\right)^s + \epsilon_{33}\,E_z = 0$$
$$E_z^s = -\frac{e_{31}}{\epsilon_{33}}\left(\frac{\partial u_0}{\partial_x} + z\,\frac{\partial_{\psi(x)}}{\partial_x}\right)^s \quad (23)$$

Based on this, the sensor stress relation is obtained as follows:

$$\sigma_{xx}^s = \left(c_{11} + \frac{e_{31}{}^2}{\epsilon_{33}}\right)\left(\frac{\partial u_0}{\partial_x} + z\,\frac{\partial_{\psi(x)}}{\partial_x}\right)^s \quad (24)$$

On this basis, by placing the electric field strength in the sensor and the experimental relation $E_i = \varphi_i$ [14] with each other and integrating into the direction of z:

$$V^s = \int_{z_2}^{z_3} E_z^s\,dz$$
$$V^s = -\frac{e_{31}\,h_s}{\epsilon_{33}}\left(\frac{\partial u_0}{\partial_x} + h_m^s\,\frac{\partial_{\psi(x)}}{\partial_x}\right)^s \quad (25)$$
$$h_m^s = \frac{z_2 + z_3}{2}$$

To obtain the governing equations of the operator, it can be assumed that the distribution of electrical potential within the operator as a second-order function [4] is given in the following relation:

$$\varphi^a = \varphi_0 + z\,\varphi_1 + z^2\,\varphi_2 \quad (26)$$

Given that potential difference is required in the operator, the following electrical boundary conditions are considered:

$$\varphi = V^a \quad at \quad z = z_0 = \frac{h}{2} + h_a$$
$$\varphi = 0 \quad at \quad z = z_1 = \frac{h}{2} \quad (27)$$

Using the above boundary conditions and using the Maxwell equation [14], the following equation will be obtained for the distribution of electrical potential:

$$\varphi^a = \varphi_0^a + z\left(\frac{V^a}{h_a} - h_m^a\,\frac{e_{31}}{\epsilon_{33}}\,\frac{\partial_{\psi(x)}}{\partial_x}\right)$$
$$+z^2\,\frac{e_{31}}{2\,\epsilon_{33}}\,\frac{\partial_{\psi(x)}}{\partial_x} \quad (28)$$

Accordingly, we will have the following relation for E_z [14]:

$$E_z = -\frac{\partial\varphi}{\partial Z} = -\frac{V^a}{h_a} + \frac{e_{31}{}^a}{\epsilon_{33}{}^a}\,(h_m^a - z)\,\frac{\partial_{\psi(x)}}{\partial_x} \quad (29)$$

Based on this, the operator stress relation will be obtained as follows:

$$\sigma_{xx}^a = c_{11}\left(\frac{\partial u_0}{\partial_x} + z\,\frac{\partial_{\psi(x)}}{\partial_x}\right)^a + e_{31}\,\frac{V^a}{h_a} \quad (30)$$

$$-\frac{e_{31}{}^{2}}{\epsilon_{33}}\,(h_m^a - z)^a\,\frac{\partial_{\psi(x)}}{\partial_x}$$

To see the effect of control on the structure, the output voltage of the sensor is related to the operating voltage with the following relation:

$$V^a = G\,V^S = -\frac{e_{31}\,h_S\,G}{\epsilon_{33}} \left(\frac{\partial u_0}{\partial_x} + h_m^s\,\frac{\partial_{\psi(x)}}{\partial_x}\right) \tag{31}$$

By placing relation (30) in relation (31) the final relation for the operator stress will be obtained:

$$\sigma_{xx}^a = c_{11}\left(\frac{\partial u_0}{\partial_x} + z\,\frac{\partial_{\psi(x)}}{\partial_x}\right)^a - \frac{e_{31}{}^{2}\,h_S\,G}{h_a\,\epsilon_{33}}\left(\frac{\partial u_0}{\partial_x} + h_m^s\,\frac{\partial_{\psi(x)}}{\partial_x}\right) - \frac{e_{31}{}^{2}}{\epsilon_{33}}\,(h_m^a - z)^a\,\frac{\partial_{\psi(x)}}{\partial_x} \tag{32}$$

Since there is no external electrical charge in the sensor, so the electrical displacement of this layer will be in the direction of zero radii, so for the sensor layer:

$$D_z = e_{13}\,\varepsilon_x + e_{23}\,\varepsilon_\theta + e_{33}\,\varepsilon_z + \epsilon_{33}\,E_z = 0 \tag{33}$$

That:

$$E_z^s = -\frac{1}{\epsilon_{33}}\,(e_{13}\,\varepsilon_x + e_{23}\,\varepsilon_\theta + e_{33}\,\varepsilon_z) \tag{34}$$

By placing the relation (32) in relation (35), the stress relations for the sensor layer will be obtained:

$$\sigma_x^s = c_{11}\varepsilon_x + c_{12}\varepsilon_\theta + c_{13}\varepsilon_z + \frac{e_{13}}{\epsilon_{33}}\,(e_{13}\,\varepsilon_x + e_{23}\,\varepsilon_\theta + e_{33}\,\varepsilon_z)$$

$$\sigma_\theta^s = c_{12}\varepsilon_x + c_{22}\varepsilon_\theta + c_{23}\varepsilon_z + \frac{e_{23}}{\epsilon_{33}}\,(e_{13}\,\varepsilon_x + e_{23}\,\varepsilon_\theta + e_{33}\,\varepsilon_z) \tag{35}$$

On this basis, by equating the intensity of the electric field in the sensor and the experimental relation $E_i = \varphi_i$ [14] together and integrating into the direction z:

$$V^s = \int_{z_0}^{z_1} E_z^s\,dz$$

$$V^s = -\frac{h_s}{\epsilon_{33}}\,(e_{13}\,\frac{\partial u_0}{\partial_x} + e_{23}\,\frac{W(x\,.\,\theta)}{R})^s \tag{36}$$

According to the shell theory, the second-order of the force and time relations of the sensor layer is defined as follows [14]:

$$N_x^s = \int_{z_1}^{z_0} \sigma_x^s \, 2\,\pi\, R_1 \, d_z$$
$$M_x^s = \int_{z_1}^{z_0} \sigma_x^s \, 2\,\pi\, R_1 \, z \, d_z \qquad (37)$$
$$N_\theta^s = \int_{z_1}^{z_0} \sigma_\theta^s \, L \, d_z$$

By placing the relation (36) in relation (37), the force and moment for the sensor layer are obtained as follows:

$$N_x^s = 2\,\pi\, R_1\, h_s \left[\left(c_{11} + \frac{e_{13}^2}{\epsilon_{33}}\right)\frac{\partial u_0}{\partial_x} + \left(c_{12} + \frac{e_{13}\, e_{23}}{\epsilon_{33}}\right)\frac{W(x.\theta)}{R}\right]$$
$$M_x^s = 2\,\pi\, R_1 \left(\frac{z_0^2 - z_1^2}{2}\right) \left[\left(c_{11} + \frac{e_{13}^2}{\epsilon_{33}}\right)\frac{\partial u_0}{\partial_x} + \left(c_{12} + \frac{e_{13}\, e_{23}}{\epsilon_{33}}\right)\frac{W(x.\theta)}{R}\right] \qquad (38)$$
$$N_\theta^s = L\, h_s \left[\left(c_{12} + \frac{e_{13}\, e_{23}}{\epsilon_{33}}\right)\frac{\partial u_0}{\partial_x} + \left(c_{22} + \frac{e_{23}^2}{\epsilon_{33}}\right)\frac{W(x.\theta)}{R}\right]$$

To obtain the equations governing the operator, it can be assumed that the distribution of the electric potential inside the operator as a function of the first order [4] is as follows:

$$\varphi^a = \varphi_0 + z\,\varphi_1 \qquad (39)$$

Given that potential difference is required in the operator, the following electrical boundary conditions are considered:

$$\varphi = V^a \quad \text{at} \quad z = z_{N+2} = \frac{-H}{2} - h_a$$
$$\varphi = 0 \quad \text{at} \quad z = z_{N+1} = \frac{-H}{2} \qquad (40)$$

Using the above boundary conditions and using the Maxwell equation [14], the following equation will be obtained for the distribution of electrical potential:

$$\varphi^a = -\frac{H\, V^a}{2\, h_a} - z\,\frac{V^a}{h_a} \qquad (41)$$

Accordingly, will have the following relation for E_z [14]:

$$E_z = -\frac{\partial \varphi}{\partial Z} = \frac{V^a}{h_a} \qquad (42)$$

To observe the effect of control on the structure, the output voltage of the sensor is related to the operating voltage with the following relation:

Technium Vol. 4, No. 7 pp.22-39 (2022)
ISSN: 2668-778X
www.techniumscience.com

$$V^a = G\,V^S = -\frac{G\ h_s}{\epsilon_{33}}\left(e_{13}\frac{\partial u_0}{\partial_x} + e_{23}\frac{W(x.\theta)}{R}\right)^s \tag{43}$$

Based on this, the operator stress ratio will be obtained as follows:

$$\begin{aligned}\sigma_x^a &= c_{11}\varepsilon_x + c_{12}\varepsilon_\theta + c_{13}\varepsilon_z \\ &+\frac{e_{13}\,G\,h_s}{h_a\,\epsilon_{33}}\left(e_{13}\frac{\partial u_0}{\partial_x} + e_{23}\frac{W(x.\theta)}{R}\right) \\ \sigma_\theta^a &= c_{12}\varepsilon_x + c_{22}\varepsilon_\theta + c_{23}\varepsilon_z \\ &+\frac{e_{23}\,G\,h_s}{h_a\,\epsilon_{33}}\left(e_{13}\frac{\partial u_0}{\partial_x} + e_{23}\frac{W(x.\theta)}{R}\right)\end{aligned} \tag{44}$$

According to shell theory, the second-order of force and time relations of the operator layer is defined as follows [14]:

$$\begin{aligned}N_x^a &= \int_{z_{N+2}}^{z_{N+1}} \sigma_x^a\, 2\,\pi\, R_2\, d_z \\ M_x^a &= \int_{z_{N+2}}^{z_{N+1}} \sigma_x^a\, 2\,\pi\, R_2\, z\, d_z \\ N_\theta^a &= \int_{z_{N+2}}^{z_{N+1}} \sigma_\theta^a\, L\, d_z\end{aligned} \tag{45}$$

By placing the relation (44) in relation (45), the force and moment for the operator layer are obtained as follows:

$$\begin{aligned}N_x^a &= 2\,\pi\,R_2\,h_a\left[\left(c_{11} + \frac{e_{13}^2\,G\,h_s}{h_a\,\epsilon_{33}}\right)\frac{\partial u_0}{\partial_x} + \left(c_{12}\right.\right. \\ &\left.\left. + \frac{e_{13}\,e_{23}\,G\,h_s}{h_a\,\epsilon_{33}}\right)\frac{W(x.\theta)}{R}\right] \\ M_x^a &= 2\,\pi\,R_2\left(\frac{z_0^2 - z_1^2}{2}\right)\left[\left(c_{11} + \frac{e_{13}^2}{\epsilon_{33}}\right)\frac{\partial u_0}{\partial_x} + \left(c_{12}\right.\right. \\ &\left.\left. + \frac{e_{13}\,e_{23}}{\epsilon_{33}}\right)\frac{W(x.\theta)}{R}\right] \\ N_\theta^a &= L\,h_a\left[\left(c_{21} + \frac{e_{13}\,e_{23\,G\,h_s}}{h_a\,\epsilon_{33}}\right)\frac{\partial u_0}{\partial_x} + \left(c_{22}\right.\right. \\ &\left.\left. + \frac{e_{23}^2\,G\,h_s}{h_a\,\epsilon_{33}}\right)\frac{W(x.\theta)}{R}\right]\end{aligned} \tag{46}$$

And for boundary conditions:

For fixed edges:

$$u_0 = v_0 = w_0 = 0,\quad \psi_x = \psi_y = 0 \ \text{ at } \ x, y = \text{const.} \tag{47-a}$$

For edges with simple support:

$$\begin{aligned}v_0 = w_0 = 0,\ \psi_y = 0,\ N_x = 0,\ M_x = 0 \ \text{at} \ x = \text{const.} \\ u_0 = w_0 = 0,\ \psi_x = 0,\ N_y = 0,\ M_y = 0 \ \text{at} \ y = \text{const.}\end{aligned} \tag{47-b}$$

Technium Vol. 4, No. 7 pp.22-39 (2022)
ISSN: 2668-778X
www.techniumscience.com

And finally for the free edges:

$$N_x = N_{xy} = 0,\ M_x = M_{xy} = 0,\ Q_x = 0 \text{ at } x = \text{const.}$$
$$N_{xy} = N_y = 0,\ M_{xy} = M_y = 0,\ Q_y = 0 \text{ at } y = \text{const.} \quad (47\text{-c})$$

3 Generalized Differential Quadrature Method (GDQM)

The first derivative of the $f(x)$ function concerning x at any point x_i is as follows:

$$f_x^{(1)}(x_i) = \sum_{j=1}^{N} H_{ij}^{(1)} f_x^{(1)}(x_j)\ ,\ i = 1, 2, ..., N \quad (48)$$

That $H_{ij}^{(1)}$ is the weighted factor derivative of the first order and N is the total number of nodes in the domain. The relation (48) is called the quadratic differential [2]. The Generalized Quadratic Differential Method (GDQM) proposed to solve the differential equations in the field of fluid dynamics was a generalization to the quadrature differential method. The standard function in this method is as follows:

$$g_k(x) = \frac{\prod_{j=1}^{N}(x - x_j)}{(x - x_k)\prod_{j=1, k\neq j}^{N}(x_k - x_j)},\ k = 1, 2, ..., N \quad (49)$$

By placing the relation (49) in relation (48), the weight coefficients will be obtained by solving the equation device as follows:

$$H_{ij}^{(1)} = \frac{\prod_{k=1, k\neq i}^{N}(x_i - x_k)}{(x_i - x_j)\prod_{k=1, k\neq j}^{N}(x_j - x_k)},\ i, j = 1, 2, ..., N;\quad i \neq j \quad (50)$$

As can be seen from Equation (50), there is no limit to the selection of nodes in this method [2]. Using the Taylor series:

$$\sum_{j=1}^{N} H_{ij}^{(1)} = 0,\ i, j = 1, 2, ..., N;\ i \neq j \quad (51)$$

With the help of relation (51):

$$H_{ii}^{(1)} = -\sum_{j=1}^{N} H_{ij}^{(1)},\ i, j = 1, 2, ..., N;\ i \neq j \quad (52)$$

The same can be done to find the weight coefficients for the second and higher-order derivatives. Here is a summary of the final results using the Shu return relation; So:

$$H_{ij}^{(r)} = r\left[H_{ij}^{(1)} H_{ij}^{(r-1)} - \frac{H_{ij}^{(r-1)}}{x_i - x_j}\right],\quad \begin{matrix} i, j = 1, 2, ..., N\ ;\ i \neq j \\ r = 2, 3, ..., N-1 \end{matrix}$$
$$H_{ii}^{(r)} = -\sum_{j=1}^{N} H_{ij}^{(r)},\quad \begin{matrix} i, j = 1, 2, ..., N\ ;\ i \neq j \\ r = 2, 3, ..., N-1 \end{matrix} \quad (53)$$

That $H_{ij}^{(r)}$ is the weight factor of the r derivative [2]. In the following, we will investigate the quadratic generalized multidimensional differential method.

3.1 Multi-dimensional generalized quadratic differential

The GDQ method can be generalized to multidimensional problems. Here we will deal with the 2D GDQ

Technium Vol. 4, No. 7 pp.22-39 (2022)
ISSN: 2668-778X
www.techniumscience.com

method. Relations for higher dimensions can simply be extracted, such as two-dimensional GDQ relations. In GDQ we have two dimensions:

$$f_x^{(n)}\left(x_i,y_j\right)=\sum_{k=1}^{N}H_{ik}^{x(n)}f\left(x_k,y_j\right)\quad \begin{matrix} i=1,2,...,N \\ j=1,2,...,M \end{matrix},\ n=2,3,...,N-1 \tag{54}$$

$$f_y^{(m)}\left(x_i,y_j\right)=\sum_{k=1}^{M}H_{jk}^{y(m)}f\left(x_i,y_k\right)\quad \begin{matrix} i=1,2,...,N \\ j=1,2,...,M \end{matrix},\ m=2,3,...,M-1 \tag{55}$$

That $f_x^{(n)}\left(x_i,y_j\right)$ is the derivative of the order *n* of the function *f* relative to *x* at the point $\left(x_i,y_j\right)$ $f_y^{(m)}\left(x_i,y_j\right)$, is also the derivative of the order m of the function *f* relative to *y* at the mentioned point and *N* and *M* are also the number of amplitude points in the direction of *x* and *y*, respectively. $H_{ik}^{x(n)}$ and $H_{jk}^{y(m)}$ will be the weight coefficients for derivatives of order *n* and *m*, respectively, in the direction of *x* and *y*. These coefficients can be achieved with the help of the following relations; So:

$$\begin{aligned} H_{ij}^{y(m)} &= m\left[H_{ij}^{y(1)}H_{ij}^{y(m-1)}-\frac{H_{ij}^{y(m-1)}}{y_i-y_j}\right], && i,j=1,2,...,M\ ;\ i\neq j \\ & && m=2,3,...,M-1 \\ H_{ii}^{y(m)} &= -\sum_{j=1}^{N}H_{ij}^{y(m)}, && i,j=1,2,...,M\ ;\ i\neq j \\ & && m=2,3,...,M-1 \end{aligned} \tag{56}$$

$$\begin{aligned} H_{ij}^{x(n)} &= n\left[H_{ij}^{x(1)}H_{ij}^{x(n-1)}-\frac{H_{ij}^{x(n-1)}}{x_i-x_j}\right], && i,j=1,2,...,N\ ;\ i\neq j \\ & && n=2,3,...,N-1 \\ H_{ii}^{x(n)} &= -\sum_{j=1}^{N}H_{ij}^{x(n)}, && i,j=1,2,...,N\ ;\ i\neq j \\ & && n=2,3,...,N-1 \end{aligned} \tag{57}$$

That:

$$\begin{aligned} H_{ij}^{x(1)} &= \frac{\prod_{k=1,k\neq i}^{N}\left(x_i-x_k\right)}{\left(x_i-x_j\right)\prod_{k=1,k\neq j}^{N}\left(x_j-x_k\right)}, && i,j=1,2,...,N\ ;\ i\neq j \\ H_{ii}^{x(1)} &= -\sum_{j=1}^{N}H_{ij}^{x(1)}, && i,j=1,2,...,N\ ;\ i\neq j \end{aligned} \tag{58}$$

$$\begin{aligned} H_{ij}^{y(1)} &= \frac{\prod_{k=1,k\neq i}^{M}\left(y_i-y_k\right)}{\left(y_i-y_j\right)\prod_{k=1,k\neq j}^{M}\left(y_j-y_k\right)}, && i,j=1,2,...,M\ ;\ i\neq j \\ H_{ii}^{y(1)} &= -\sum_{j=1}^{M}H_{ij}^{y(1)}, && i,j=1,2,...,M\ ;\ i\neq j \end{aligned} \tag{59}$$

The GDQ method can be used to solve ordinary and partial differential equations. The use of this method in static problems of the algebraic equivalent device will result in the unknowns being the same as the dependent values at the node points. In dynamic matters, the unknowns will be time-dependent values at the nodes.The desired accuracy and stability of the results are obtained by distributing the Chebyshev-Gauss-Lobatto node points [15]; so:

Technium Vol. 4, No. 7 pp.22-39 (2022)
ISSN: 2668-778X
www.techniumscience.com

$$x_i = \frac{L}{2}\left[1-\cos\left(\frac{i-1}{N-1}\cdot\pi\right)\right], \quad i=1,2,...,N$$
$$y_j = \frac{W}{2}\left[1-\cos\left(\frac{j-1}{M-1}\cdot\pi\right)\right], \quad j=1,2,...,M \tag{60}$$

(1)

4 Results and discussion

In this section, for example, the problem solved using the analytical method in the reference [1] is used and for a two-layer composite [0/90] [1]:

$$a=b=25\text{ cm}, \quad h=1\text{ cm}$$
$$\rho=8\times10^{-6}\text{ Ns}^2/\text{cm}^4, \quad E_2=2.1\times10^6\text{ N/cm}^2$$
$$E_1=25E_2, \quad G_{12}=G_{13}=0.5E_2, \quad G_{23}=0.2E_2, \nu_{12}=0.25 \tag{61}$$

The boundary conditions used in this problem are simple for the four sides of the support. Figure 3 shows the dimensionless displacement for a wide sinusoidal load that is suddenly inserted into the plate.

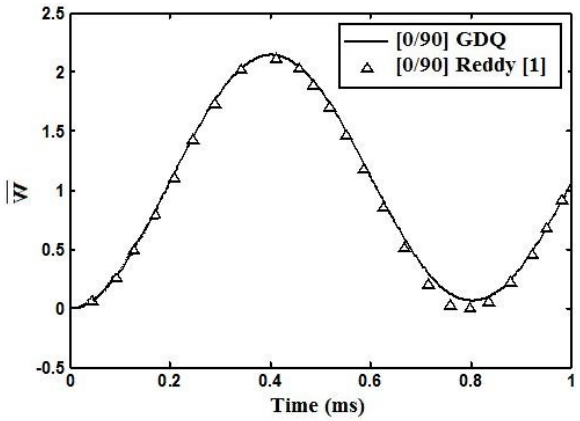

Immediate deformation in the center of the plate over time for the extensive sinusoidal load.

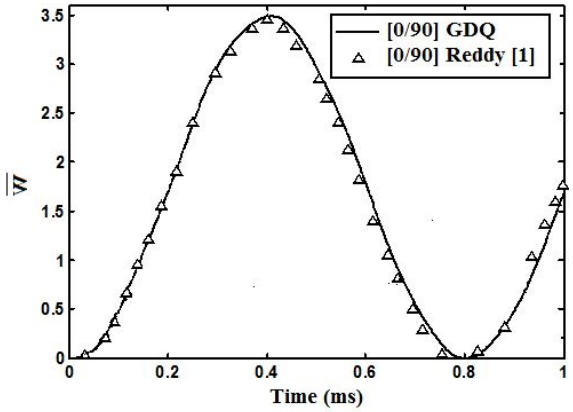

Immediate deformation in the center of the plate over time for uniform pressure.

Figure 3. The dimensionless displacement for a wide sinusoidal load.

Technium Vol. 4, No. 7 pp.22-39 (2022)
ISSN: 2668-778X
www.techniumscience.com

In which the latent sinusoidal force is defined as follows [1]:

$$q(x,y,t)=q_0(t)\sin\left(\frac{\pi x}{a}\right)\sin\left(\frac{\pi y}{b}\right) \tag{62}$$

That $q_0(t)=1800$ is considered. Deformation can be achieved without the following relation [1]:

$$\bar{w}=100\,w\left(\frac{E_2h^3}{q_0a^4}\right) \tag{63}$$

Figure 4 shows the dimensionless displacement for a uniform pressure that suddenly enters the plate. As shown in Figures 3 and 4, the results obtained by the GDQ method are in good agreement with the results of the analytical solution presented in the reference [1]. These figures show the free vibration of the plate for the extensive load that enters the plate as a step (sudden) function. For both figures, the maximum values of displacement occurred at 0.4 and 0.8 seconds. The effect of increasing the number of composite layers on the first natural frequency is indistinguishable for the same total thickness and for and in the lay-up mode. Due to the same thickness of the layers, as the number of composite layers increases and the total thickness is constant, Frequency changes were very small compared to other piezoelectric coefficients, and their diagrams were neglected. Figure 3 shows that as the value of the positive electric potential increases, the natural frequency of the sheet decreases. Table 1 shows is the effect of the plate thickness on the dimensionless natural frequency of the studied smart plate ($V_{CNT}=0.17$, $\Delta T=0$).

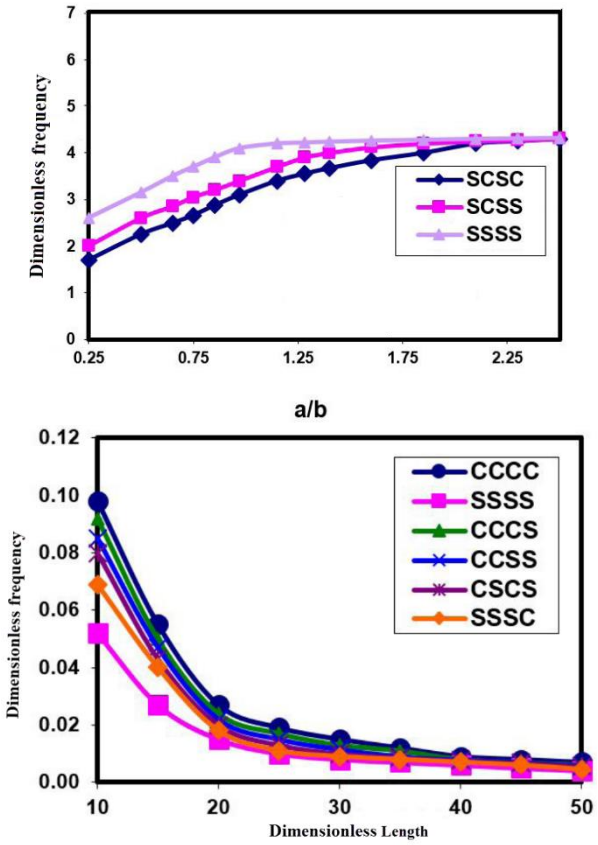

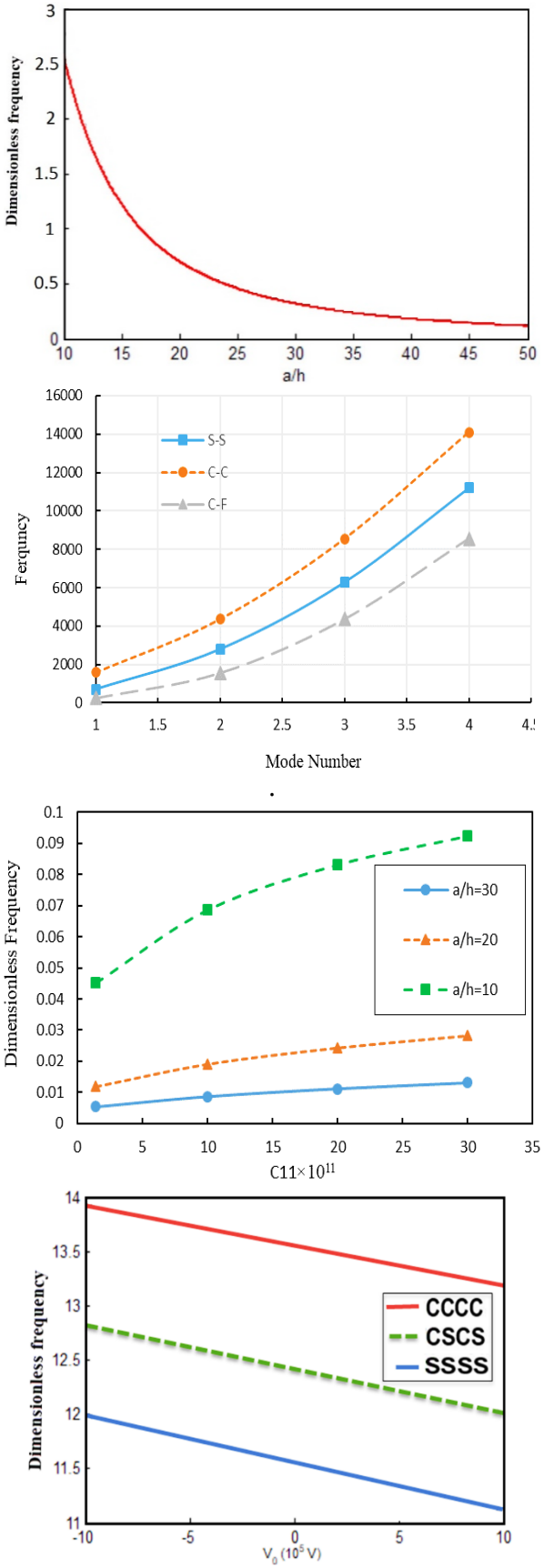

Figure 4. The dimensionless frequency for a uniform pressure at the plate.

Table 1. Effect of the plate thickness on the dimensionless natural frequency of the studied smart plate ($V_{CNT} = 0.17, \Delta T = 0$) [14].

Thickness, *h*		Electric
0.0001	0.1	potential, *v*
0.108602	0.105776	-100
0.105773	0.105773	0
0.102866	0.105770	+100

5 Conclusion

This paper investigated the free vibration analysis of an electromechanical system consisting of a three-layer sheet. The three-layer sandwich sheet consists of a calibrated core and is equipped with two piezoelectric calibrated layers. The equations of motion are based on first-order shear theory. Considering the above results, to increase the safety of the sheet against the phenomenon of resonance and to raise the natural frequency, the following suggestions are presented for the design of composite nanofibers. As much as possible, the sheet to be designed should have a lower side-to-thickness ratio. Negative electric potential and positive magnetic potential increase natural frequency.

References

[1] Han, Jae-Hung, and In Lee. "Analysis of composite plates with piezoelectric actuators for vibration control using layerwise displacement theory." Composites Part B: Engineering 29, no. 5 (1998): 621-632. https://doi.org/10.1016/S1359-8368(98)00027-4

[2] Narayanan, S., and V. Balamurugan. "Finite element modelling of piezolaminated smart structures for active vibration control with distributed sensors and actuators." Journal of sound and vibration 262, no. 3 (2003): 529-562. https://doi.org/10.1016/S0022-460X(03)00110-X

[3] Heidary, Fariborz, and M. Reza Eslami. "Piezo-control of forced vibrations of a thermoelastic composite plate." Composite structures 74, no. 1 (2006): 99-105. https://doi.org/10.1016/j.compstruct.2005.03.011

[4] Kargarnovin, M. H., M. M. Najafizadeh, and N. S. Viliani. "Vibration control of a functionally graded material plate patched with piezoelectric actuators and sensors under a constant electric charge." Smart materials and structures 16, no. 4 (2007): 1252. https://www.sid.ir/en/journal/ViewPaper.aspx?ID=293982

[5] Zhang, L. W., Z. G. Song, and K. M. Liew. "Optimal shape control of CNT reinforced functionally graded composite plates using piezoelectric patches." Composites Part B: Engineering 85 (2016): 140-149. https://doi.org/10.1016/j.compositesb.2015.09.044

[6] Sharma, Anshul, Anuruddh Kumar, C. K. Susheel, and Rajeev Kumar. "Smart damping of functionally graded nanotube reinforced composite rectangular plates." Composite Structures 155 (2016): 29-44. https://doi.org/10.1016/j.compstruct.2016.07.079

[7] Ansari, R., R. Gholami, and A. Norouzzadeh. "Size-dependent thermo-mechanical vibration and instability of conveying fluid functionally graded nanoshells based on Mindlin's strain gradient theory." Thin-Walled Structures 105 (2016): 172-184. https://doi.org/10.1016/j.tws.2016.04.009

[8] Farzam-Rad, S. Amir, Behrooz Hassani, and Abbas Karamodin. "Isogeometric analysis of functionally graded plates using a new quasi-3D shear deformation theory based on physical neutral surface." Composites Part B: Engineering 108 (2017): 174-189.

https://doi.org/10.1016/j.compositesb.2016.09.029
[9] Chen, W. Q., Z. G. Bian, and H. J. Ding. "Three-dimensional vibration analysis of fluid-filled orthotropic FGM cylindrical shells." International Journal of Mechanical Sciences 46, no. 1 (2004): 159-171.
https://doi.org/10.1016/j.ijmecsci.2003.12.005
[10] Safarpour, M., A. R. Rahimi, and A. Alibeigloo. "Static and free vibration analysis of graphene platelets reinforced composite truncated conical shell, cylindrical shell, and annular plate using theory of elasticity and DQM." Mechanics Based Design of Structures and Machines 48, no. 4 (2020): 496-524.
https://doi.org/10.1080/15397734.2019.1646137
[11] Habibi, Mostafa, Davoud Hashemabadi, and Hamed Safarpour. "Vibration analysis of a high-speed rotating GPLRC nanostructure coupled with a piezoelectric actuator." The European Physical Journal Plus 134, no. 6 (2019): 1-23.
https://doi.org/10.1140/epjp/i2019-12742-7
[12] Ebrahimi, Farzad, Eris Elianddy Bin Supeni, Mostafa Habibi, and Hamed Safarpour. "Frequency characteristics of a GPL-reinforced composite microdisk coupled with a piezoelectric layer." The European Physical Journal Plus 135, no. 2 (2020): 144.
https://doi.org/10.1140/epjp/s13360-020-00217-x
[13] Ramegowda, Prakasha Chigahalli, Daisuke Ishihara, Rei Takata, Tomoya Niho, and Tomoyoshi Horie. "Finite element analysis of a thin piezoelectric bimorph with a metal shim using solid direct-piezoelectric and shell inverse-piezoelectric coupling with pseudo direct-piezoelectric evaluation." Composite Structures 245 (2020): 112284.
https://doi.org/10.1016/j.compstruct.2020.112284
[14] Tiersten, Henry Frank. Linear Piezoelectric Plate Vibrations: Elements of the Linear Theory of Piezoelectricity and the Vibrations Piezoelectric Plates. Springer, 2013.
[15] Kim, Seonhee, and Sang Dong Kim. "Preconditioning on high-order element methods using Chebyshev–Gauss–Lobatto nodes." Applied numerical mathematics 59, no. 2 (2009): 316-333.
https://doi.org/10.1016/j.apnum.2008.02.007

Submitted: 03.05.2022
Revised: 11.07.2022
Accepted: 02.08.2022